Article

A Novel Resistive Sensor Network Utilizing an SAP-Enhanced Ionic Layer and CNT Doping for Multipoint Pressure Measurement

Leijin Fan, Yuantao Liu, Xiaofeng Yang,* and Hu Sun*

Read Online

ACCESS | Metrics & More | Article Recommendations | Supporting Information

ABSTRACT: Amidst the rapid advancements in flexible electronics, flexible pressure sensors have achieved widespread applications in fields such as wearable devices and motion monitoring. Nevertheless, it is still a challenge to design a sensor with high sensitivity, cost-effectiveness, and a simplified manufacturing process. This paper introduces a piezoresistive sensor built upon a composite conductive filler. The sensor incorporates a super absorbent polymer (SAP) to absorb a phosphoric acid solution and doped carbon nanotubes as the composite conductive filler. In contrast to conventional rigid conductive fillers, the elastic polymer SAP enhances the sensor's stability significantly by exhibiting superior compatibility with the polydimethylsiloxane matrix, all the while reducing its Young's modulus. This work aims to theoretically elucidate the underlying principles that enable the sensor to achieve high sensitivity. It focuses on the induction of charge carriers due to pressure, which leads to the formation of a conductive pathway and subsequent changes in resistance, thus facilitating precise pressure detection. The paper also discusses the effects of piezoresistive layers with varying thicknesses and conductive fillers on the sensor's output performance. The results highlight the sensor's high sensitivity (0.094 kPa^{-1}), rapid response time (105 ms), and exceptional cyclic load/unload stability (>5000 cycles). Furthermore, this paper establishes a versatile sensing network by integrating a portable inductance, capacitance, and resistance instrument with a programmable logic controller module. Compared to individual sensors, this system enables multipoint measurements, offering high spatial resolution and real-time monitoring capabilities, significantly expanding its overall practicality.
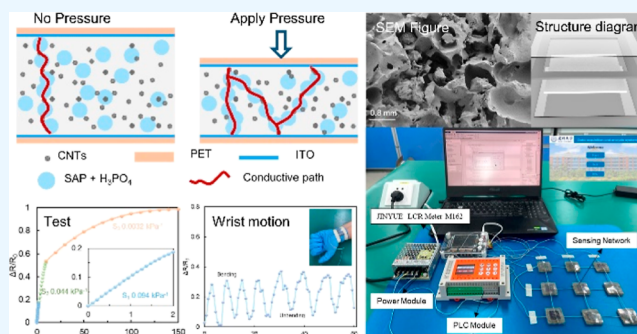
1. INTRODUCTION

Pressure sensing technology is essential in a multitude of scenarios, encompassing physical signal detection and monitoring.[1,2] While rigid single-point sensors like load cells have achieved maturity in terms of high accuracy and stability over the years, they often face limitations related to spatial arrangement and installation due to their bulky size. In recent years, the development of micro-/nanomaterials and design strategies has led to burgeoning interest in endowing pressure sensors with flexibility and high spatial resolution characteristics. At the same time, the research of metamaterials with negative permeability, negative dielectric constant media, and 3D printing technology has also promoted the change.[3−5] This trend has gained prominence not only in cutting-edge technology applications (e.g., robotic haptics, prosthetics, human−computer interfaces, wearable medical devices, etc.) but also holds the potential to supplement or replace traditional single-point sensors.[6−8]

Flexible pressure sensors offer the advantage of being easily adaptable to various surfaces, thereby reducing discomfort during measurements. The sensor array configuration enhances the spatial pressure distribution perception, enabling richer data acquisition. Flexible pressure sensors employ various mechanisms to convert pressure into electrical signals, including piezoresistive, capacitive, piezoelectric, and triboelectric principles.[9−12] Piezoelectric and triboelectric sensors exhibit high sensitivity to dynamic pressure but necessitate complex electronic designs and may introduce inaccuracies with static pressure. In scenarios requiring simultaneous measurements of static and dynamic pressures, capacitive and piezoresistive sensors are often preferred. While capacitive sensors can achieve high sensitivity and stability, they are susceptible to issues related to parasitic capacitance and noise. In contrast, piezoresistive sensors offer advantages such as straightforward fabrication, simple readout circuitry, low cost, and robust resistance to electrical interference.[13]

Piezoresistive sensors function by converting pressure into a change in resistance, which can be measured in various

configurations, such as being sandwiched between positive and negative electrodes or placed on coplanar electrodes with control over vertical or transverse resistors. Resistance comprises both volume resistance and contact resistance.[14,15] The former is influenced by material properties, including geometry and internal electrical characteristics, while the latter is related to the contact area and interface between the material and the electrode. To enhance sensor performance, extensive research has been conducted on various materials and sensing structures.

Polymer composites have garnered significant attention as promising materials for piezoresistive sensors, especially in the context of large-area and flexible sensor devices.[16,17] Typically, polymer composites consist of a plastic matrix and a conductive component. In such composites, the volume resistance is contingent on geometry and the conductive pathways within the material, phenomena elucidated by seepage theory and tunneling effects.[18,19] Percolation theory elucidates pressure-induced percolation paths formed by conductive elements, while tunneling effects involve charge carriers conducting electricity via tunneling without a physical particle-to-particle contact. Elastic substrates commonly include polymers like PDMS, PU, and TPU, while hydrogels are preferred for applications necessitating biocompatibility.[20−23] Conductive components encompass carbon-based materials, metallic materials, as well as other materials such as MXene, PPy, and PANI.[24−26]

For instance, Shi et al. introduced a pressure sensor utilizing sea-urchin-like hollow carbon spheres with extremely low load in a PDMS matrix fabricated through spin coating. This sensor capitalizes on the tunneling effect, delivering exceptional sensitivity. Even minute amounts of filler material confer the sensor with desirable attributes such as high transparency, elasticity, biocompatibility, and ease of manufacturing.[27] Moreover, the hollow structure contributes to the thermal stability. Tang et al. proposed a soft porous composite pressure sensor produced via 3D printing technology by adjusting ink composition ratios, comprising conductive carbon nanotubes (CNTs), insulating silica nanoparticles, and silicon elastomer polymers. The sensor can be tuned to exhibit negative or positive piezoresistive effects.[28] However, the above methods have some problems such as a complex preparation process and poor economy.

Apart from material selection and proportions, the sensor performance can be further enhanced by incorporating a three-dimensional microstructure on its surface. These microstructures augment mechanical properties such as compressibility and stress concentration while altering the contact area of the conductive interface, thereby improving pressure-sensing capabilities. When microstructures are designed, both regular and irregular surface morphologies can be employed. Regular surface structures encompass microbodies, microconical bodies, microcolumn arrays, and truncated conical surface structures, among others.[29−32] These structures heighten sensitivity by increasing the contact area under pressure. They can be fabricated through methods such as casting or coating onto a template, which can itself be prepared using techniques like lithography and laser engraving, commonly employing a silica template.[33,34]

Furthermore, additional surface morphologies can be integrated into the 3D structure to further enhance performance. For example, Yao et al. developed a piezoresistive sensor featuring a microconical elastomer coated with a cracked metal film. To create these cracks, they deposited a layer of platinum film with a microconical surface structure onto the PDMS substrate.[35] Li et al. also contend that combining sharp microstructures with short electrode channel lengths can enhance the sensitivity of piezoresistive pressure sensors. As a result, they constructed a sensor featuring sharp microcone structures and short channels with coplanar gold electrodes.[31]

Irregular surface structures have also piqued researchers' interest, including wrinkles, designs inspired by natural biological materials such as leaves, and configurations inspired by human skin with randomly distributed spines, akin to sandpaper.[36−38] These irregular surface structures increase the contact area and enhance the sensor's overall performance. Irregular surface structures, while often offering superior performance, may not match regular structures in terms of controllability, uniformity, and scalability for mass production. Hence, the challenge remains to develop a cost-effective, environmentally friendly, and easily manufacturable piezoresistive sensor with high sensitivity.

In this paper, a resistive pressure sensor based on a super absorbent polymer (SAP), phosphoric acid liquid, and CNT composite conductive filler is developed, and its easy preparation process is introduced. The use of elastic polymer SAP instead of the common rigid conductive filler can be better combined with the base material PDMS, which greatly improves the stability of the sensor and reduces the Young's modulus of the sensor. This paper also describes the working mechanism of the sensor and discusses the influence of different parameters on the performance of the sensor. In addition, a flexible sensor network is built to further improve the application of the system.

2. EXPERIMENTAL SECTION

2.1. Materials. SAP was acquired from Shandong Yousuo Chemical Technology Co., Ltd. (Linyi, China). Deionized water was purchased from Shanghai Acmec Biochemical Co., Ltd. (Shanghai, China). CNTs with diameters ranging from 20 to 40 nm were procured from Shanghai McLean Biochemical Co., Ltd. (Shanghai, China). Polyethylene terephthalate (PET) films were procured from Shanghai Jinpan Biotechnology Co., Ltd. (Shanghai, China). Nano indium tin oxide (ITO) powder was sourced from Guangzhou Hongwu Material Technology Co., Ltd. (Guangzhou, China). PDMS (SYLGARD 184) was obtained from Dow Corning Co., Ltd., USA. The 3 M epoxy resin adhesive was provided by Guangzhou Pen Star Technology Co., Ltd. (Guangzhou, China). Phosphoric acid was supplied by Sinopharm Chemical Reagent Co., Ltd. (Shanghai, China). The PTFE mold was purchased from Chengdu Senfa Rubber and Plastic Co., Ltd. (Chengdu, China). All materials were used as received without any additional processing or purification.

2.2. Preparation Process of the Pressure Sensor. The novel polymer material, SAP, boasts robust hydrophilic properties and exhibits certain cross-linking capabilities. When water is absorbed, it swells, maintaining excellent water retention even under compression. This study utilized SAP as an electrolyte carrier to create a conductive filler. Initially, a mixture of phosphoric acid reagent and deionized water is prepared in specific proportions, diluted, and then absorbed by SAP. Subsequently, a predefined quantity of CNTs is introduced to form the conductive filler. PDMS is then blended in a 10:1 ratio, and varying proportions of the conductive filler are gradually incorporated. Mechanical stirring
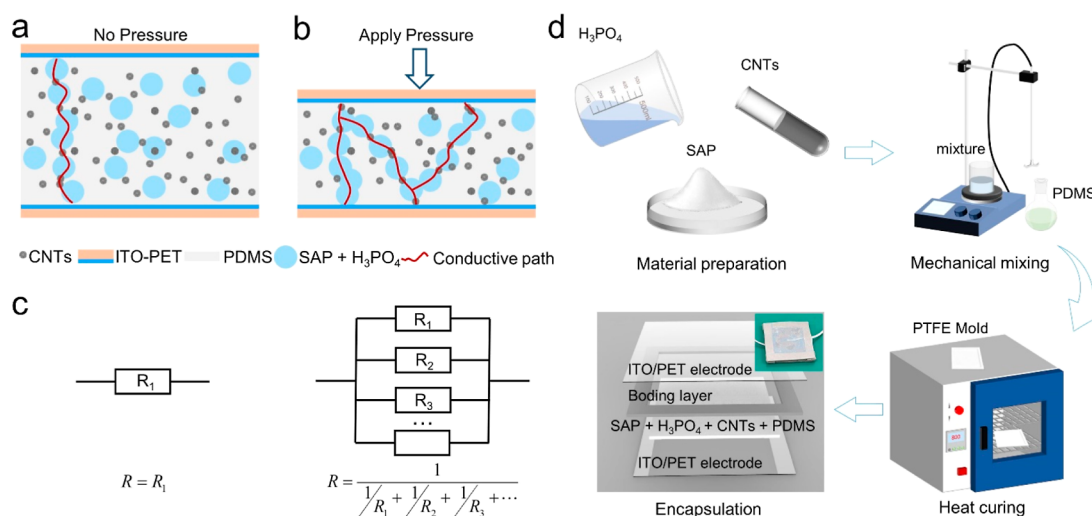
Figure 1. Sensing mechanism and fabrication process of composite conductive filler sensors. (a) No pressure. (b) Under pressure. (c) Equivalent resistance diagram. (d) Fabrication process diagram.

at room temperature for 1 h ensures even dispersion of the conductive filler within the PDMS. Finally, the mixture is cast into a PTFE mold and cured at 70 °C for 3 h to fabricate the piezoresistive layer.

For the flexible pressure sensor, an ITO/PET film is deposited using a magnetron sputtering process to serve as the electrode. A 3 M adhesive is applied as the upper and lower electrode bonding layers for the pressure sensor. A 20 mm × 20 mm sensing area is affixed to the surface of the ITO/PET electrode. The piezoresistive layer is then positioned onto the sensing area atop the ITO/PET electrode, and another layer of the ITO/PET electrode is added to assemble the pressure sensor.

2.3. Characterization and Sensing Performance Measurements. In this study, the microstructure of the piezoresistive composite conductive fillers was examined by using scanning electron microscopy (SUPRA 55, Zeiss, Germany). The crystal structure of the conductive packing was analyzed by using X-ray diffractometry (XRD-7000, Shimadzu, Japan). Fourier infrared spectroscopy (Nicolet-500, Thermo Fisher Technologies, USA) was employed to investigate the functional groups present in the conducting fillers. Resistance measurements of the sensors were conducted by utilizing a digital source instrument (2400, KEITHLEY, USA) in conjunction with a portable LCR meter (M162, JINYUE, China). The application of pressure load to the sensors was accurately accomplished by using an electronic universal testing machine (E43.104, MTS, China).

3. RESULTS AND DISCUSSION

3.1. Sensing Principle and Design Method of the Sensor. The piezoresistive layer of the sensor proposed in this paper consists of various materials, including a PDMS matrix, SAP resin, phosphoric acid, and a composite conductive filler containing CNTs. When the content of the composite conductive filler reaches a certain threshold, it leads to the formation of a conductive network, which significantly reduces the resistance of the sensor. Currently, two main theories are employed to explain the formation of these conductive networks: percolation theory and the quantum tunneling effect.[39,40]

Percolation theory posits that as the matrix undergoes deformation, the relative positions of the conductive filler particles dispersed within the matrix change. With an increase in the concentration of the conductive filler and a decrease in the average spacing, adjacent conductive particles come into contact, thereby forming a conductive path. As the number of conductive paths increases, they eventually form a complete and interconnected conductive network within the substrate. This theory demonstrates that when subjected to stress, the contact area between the conductive fillers increases, resulting in the formation of more conductive pathways and a consequent reduction in the sensor resistance.

Conversely, the tunneling effect asserts that even when conductive filler particles are not physically in direct contact with each other, they are still sufficiently close to facilitate a conductive network through electronic transitions during thermal fluctuations. Consequently, under conditions of minimal strain, substantial physical contact between conductive fillers may not be present, yet the sensor's resistance still exhibits significant changes.

To delve deeper into explaining the sensor's performance, the Debye length theory can be applied. The Debye length is a length scale that describes the diffusion of charge in a medium, and it is influenced by the electrolyte concentration and the dielectric constant of the medium.[41]

First, the charge carriers in conductive fillers typically consist of electrons or ions. The mobility of these charge carriers within conductive materials is restricted by charge diffusion.[42] The Debye length serves as a crucial parameter that is intricately linked to the electrolyte concentration and dielectric constant. A smaller Debye length indicates a broader range of interactions between charge carriers, whereas a larger Debye length signifies a more limited range of interactions.[43]

In the sensor's operation, pressure is applied, causing the charge carriers within the conductive filler to move and establish a conductive pathway. The Debye length's size impacts the interactions between these charge carriers. When the Debye length is small, applying pressure enables charge carriers to move closer to each other, facilitating the formation of conductive paths due to the extended range of interactions between them. This results in a rapid reduction in resistance.
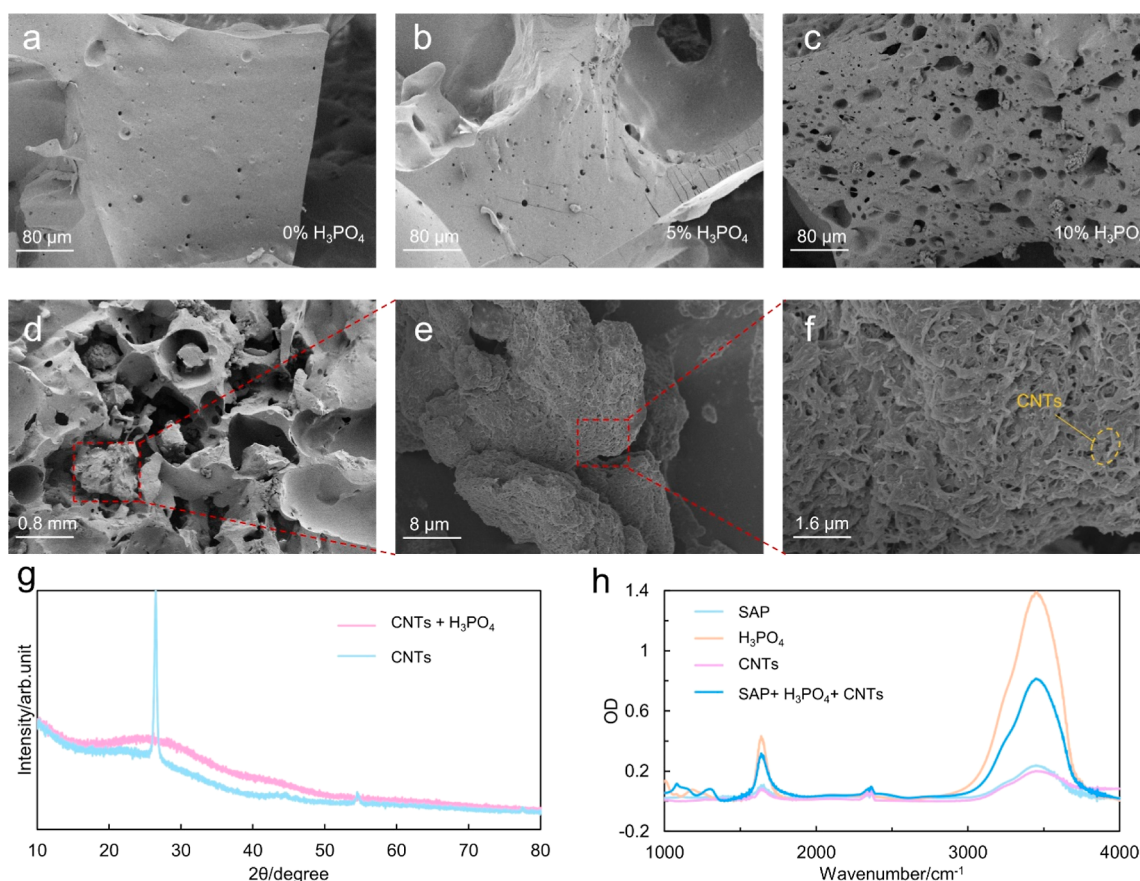
Figure 2. Multimodal characterization of the pressure sensor with composite conductive fillers. It includes SEM images of PVA absorbing different proportions of phosphoric acid (a−c), SEM images of composite conductive fillers doped with CNTs (d−f), XRD tests (g), and Fourier infrared spectroscopy tests (h).

Conversely, with a larger Debye length, the interaction range between charge carriers is more confined, necessitating greater external forces to establish a conductive channel. This elucidates why resistance can still undergo significant changes at low pressure or under conditions of minimal strain as charge carriers can still form a limited yet efficient conductive pathway through electron transitions when the Debye length is large.

As depicted in Figure 1a, the composite conductive filler is uniformly distributed within the PDMS matrix. When pressure is applied to the sensor, as illustrated in Figure 1b, the contact area between the conductive fillers increases, leading to the formation of additional conductive pathways and a subsequent reduction in the sensor resistance. Once the pressure load is removed, the sensor returns to its initial state due to the excellent elasticity of the PDMS. The equivalent circuit representing this change process is shown in Figure 1c.

Figure 1d shows an optical image of the preparation of a piezoresistive sensor comprising an ITO/PET electrode, a composite conductive filler, and a boding layer. The specific production process is described in the Experimental Section.

3.2. Multimodal Characterization of Flexible Piezoresistive Sensors. During the sensor fabrication process, it is crucial to consider the drying step, as metal salt ions tend to precipitate and crystallize, losing their conductivity, as illustrated in Figure S1. However, phosphoric acid does not suffer from this issue, as it can be mixed with water in any proportion without losing its conductive properties.

As evident in the SEM images in Figure 2a−c, the morphology of the composite conductive filler undergoes significant changes with an increasing mass fraction of phosphate, leading to an increase in pore formation. Notably, when the phosphoric acid solution's concentration is 10%, the composite conductive filler exhibits uniform and well-defined pores. Consequently, the absorption of phosphoric acid solution by SAP is optimized at this 10% concentration. After the incorporation of CNTs, the SEM images in Figure 2d−f demonstrate that CNTs are uniformly dispersed within SAP, which has absorbed the phosphoric acid ionic liquid. This distribution further enhances the sensor's performance. The change of the conductive path before and after pressure is applied is shown in Figure S2. Before pressure is applied, there are more pores in the piezoresistive layer of the sensor, and there is no conductive path between these pores. After applying pressure, part of the pores are squeezed and filled, thus forming more conductive paths in the piezoresistive layer of the sensor, which is consistent with the analytical diagram of the sensing mechanism.

Figure 2g displays the XRD pattern of a mixture containing pure CNTs and CNTs with phosphoric acid. The figure reveals that the introduction of phosphoric acid leads to the disappearance of the peaks in the XRD analysis of CNTs. This phenomenon can be attributed to the chemical interaction between phosphoric acid and CNTs, resulting in structural changes within the CNTs. These structural alterations may encompass the introduction of functional
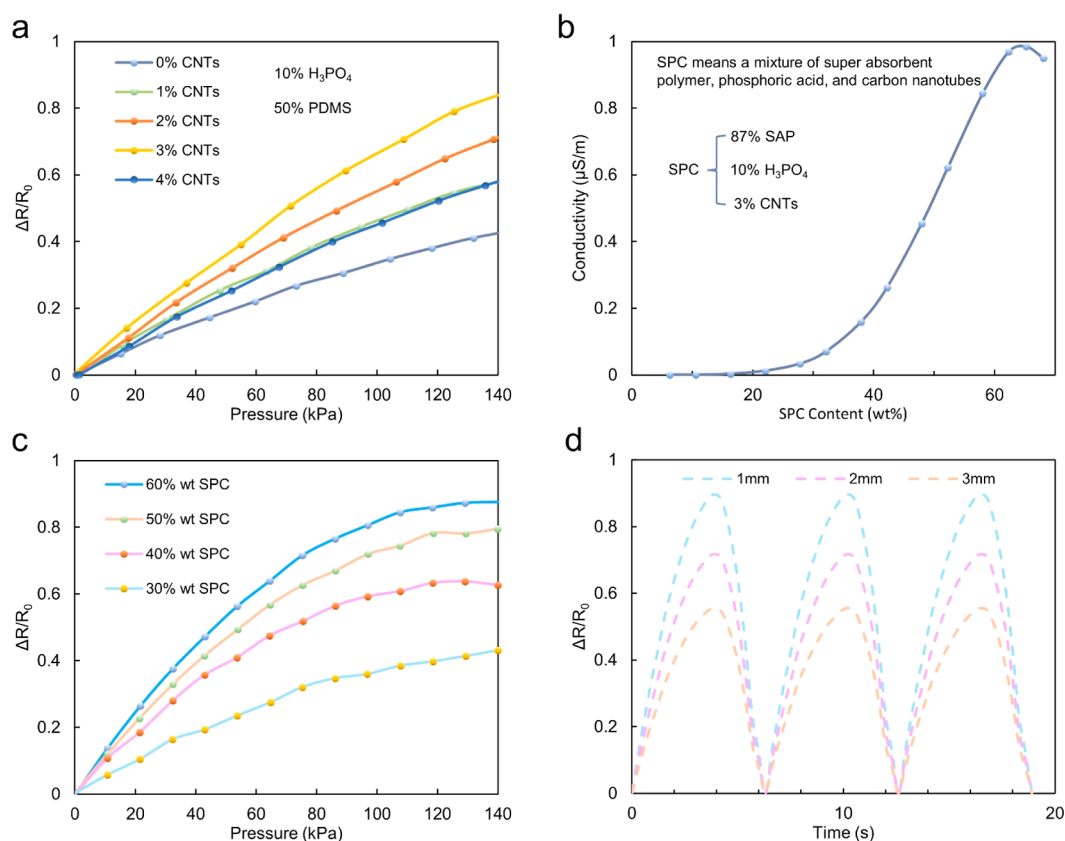
Figure 3. Performance change patterns of flexible pressure sensors. (a) Influence of CNT doping on the composite conductive filler sensor. (b) Relationship between the measured electrical conductivity of composites and conductive fillers. (c) Responsiveness of the resistance in the composite conductive layer with varying SPC contents under applied pressure. (d) Resistance output curve of the 1−3 mm composite conductive layer at 80 kPa.

groups onto the surface of the CNTs or the disruption of certain structural units within the CNTs. Moreover, phosphoric acid has the capacity to introduce functional groups onto the CNT surface, thereby modifying the chemical properties of the CNT surface. This surface modification can potentially diminish the crystallinity of the CNTs, consequently influencing the outcomes of the XRD tests. The vanishing peaks may be attributed to the irregular crystal structure or the loss of crystallinity subsequent to surface modification of the CNTs.

The Fourier infrared spectrum of SAP is depicted in Figure 2h when SAP absorbs a phosphoric acid aqueous solution and undergoes CNT doping. The composite conductive fillers exhibit distinct absorption peaks or characteristics in the Fourier infrared spectrum, setting them apart from the spectrum of untreated SAP. The incorporation of phosphoric acid ionic liquid and the introduction of CNTs induce alterations in the chemical properties of the composite conductive filler's surface. This can involve the introduction of functional groups or modifications in surface charge within the spectral wavelength range of 1000−1500. These surface modifications are manifested in FTIR spectroscopy with the emergence of new absorption peaks or changes in peak intensities.

3.3. Rule Analysis of Different Parameter Sensors. To investigate the impact of varying CNTs' doping concentrations on the piezoresistive sensor's performance, SEM images were employed to analyze the material structure under different CNT concentrations. In this study, SAP absorbed a 10%

concentration of phosphoric acid solution and PDMS with a 50% concentration. The experimental results are illustrated in Figure 3a.

As the concentration of CNTs increased, the sensor's performance exhibited a trend of initially improving and then declining. The optimal sensing performance was observed when the CNT concentration reached 3%. At lower concentrations, CNT dispersion was more uniform, but the electronic pathways between CNTs were not sufficiently connected, resulting in relatively low conductivity and elevated resistance, which adversely affected the sensor's performance. However, when the CNTs' concentration reached 3%, it is plausible that the distribution of CNTs reached an equilibrium state, enabling the formation of effective electronic pathways between them. Consequently, electrons could flow more freely between CNTs, enhancing the material's conductivity. In this scenario, the sensor exhibited its best performance, effectively detecting external pressure changes and efficiently transmitting signals.

At higher concentrations, CNTs may begin to aggregate excessively, forming large clumps or clusters. This aggregation can disrupt or irregularize the electronic pathways between CNTs, leading to a reduced conductivity. As a result, the sensor's performance may begin to deteriorate due to the restricted flow of electrons. Hence, precise control of the CNTs' concentration is crucial for achieving optimal conductivity and, in turn, enhancing the performance of piezoresistive sensors.
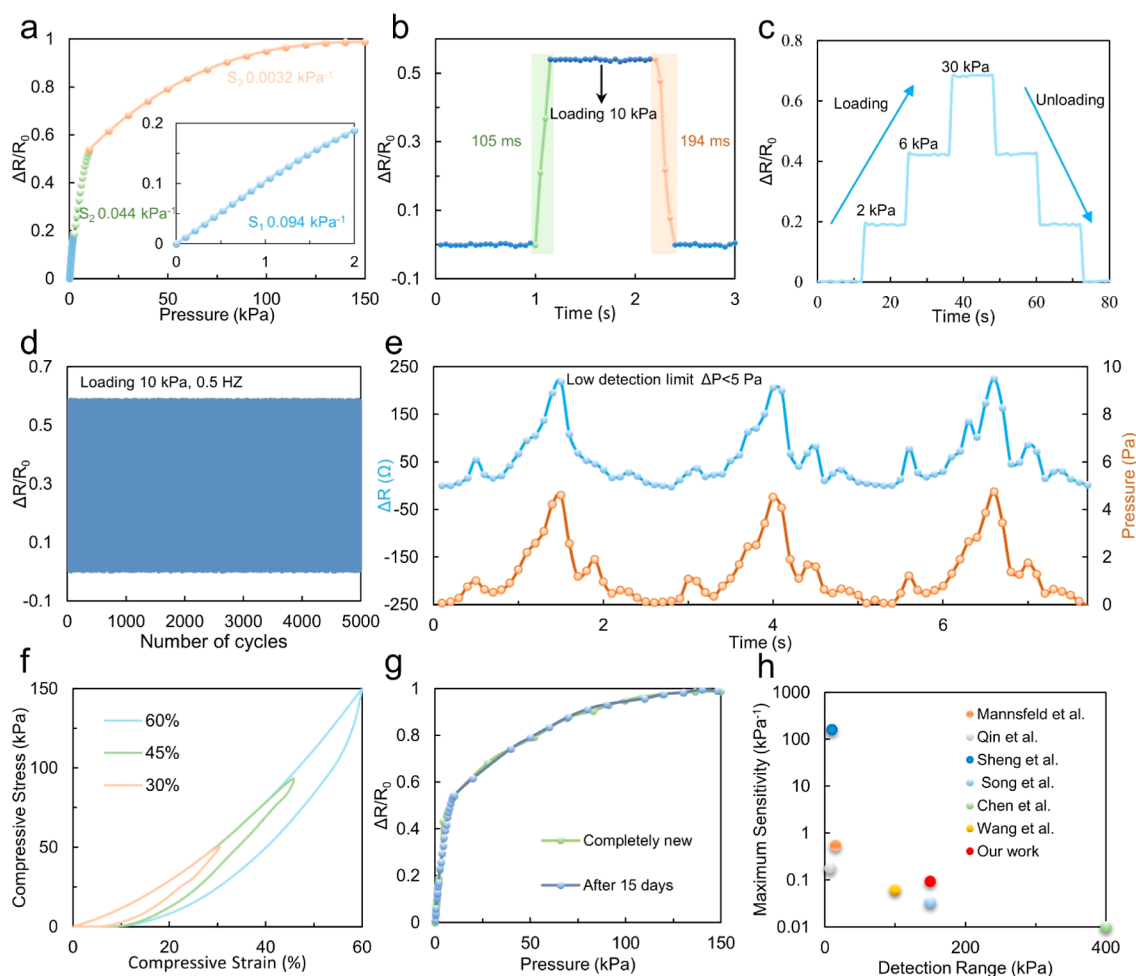
Figure 4. Characterization of piezoresistive pressure sensor sensing performance. (a) Curve of sensor sensitivity with applied pressure in the measurement range of 150 kPa. (b) Response time and relaxation time of the sensor to the pressure stimulus. (c) Response curve of the resistance change rate with time in static loading and unloading tests. (d) The durability of the sensor can be measured up to 5000 times. (e) The measurement response limit of pressure sensors is as low as 5 Pa. (f) Compressive stress−strain curves of the composite conductive layer at 30−60% different strains. (g) Comparison of the sensitivity test results of the sensor and the new sensor half a month after preparation. (h) The pressure sensing parameters of the proposed sensor are compared with those reported in the literature, including sensitivity and pressure detection range.

Figure 3b illustrates the relationship between the conductivity of the composite conductive filler and the SPC mass fraction. The SPC concentration varies from 0 to 70 wt %, with a step size of 10 wt %. In the insulation zone (0−30 wt %), the concentration of conductive fillers is low, resulting in the composite material remaining in an insulating state. This is because it fails to form a complete and interconnected internal conductive network. Transitioning to the seepage zone (30−60 wt %), the concentration of conductive fillers becomes sufficiently high to establish numerous conductive pathways, thereby connecting the material into a comprehensive conductive network. Consequently, the composite material shifts from an insulating state to displaying some level of conductivity. As the concentration of the conductive filler increases further, the composite's conductivity experiences a rapid growth, eventually reaching the threshold of percolation at 60 wt %. In the saturation region (>60 wt %), the conductive network has essentially linked the entire interior of the composite material. Newly formed conductive pathways gradually diminish the impact of the conductive network. At this stage, as the concentration of the conductive filler continues to increase, the composite material's conductivity

reaches a state of saturation. It is noteworthy that when the SPC content exceeds 70 wt %, PDMS curing becomes challenging. This characterization underscores the importance of precisely controlling the SPC mass fraction to attain the desired conductivity in the composite material while avoiding excessive SPC content that may hinder the curing process of PDMS.

To investigate the impact of varying proportions of the SPC composite conductive filler on the performance of the piezoresistive layer, as depicted in Figure 3c, it becomes evident that within the seepage zone, increased SPC content leads to improved electrical conductivity. Remarkably, at a SPC content of 60 wt %, which corresponds to the optimal conductivity of the composite filler, the sensor exhibits its peak sensing performance. The prepared sample has excellent repeatability, as shown in Figure S3. The strategies for sample preparation reproducibility are shown in the Supporting Information. Furthermore, to explore the influence of the thickness of the conductive composite layer, SPC, on the sensor's resistance output, the resistance output curve of the 1−3 mm conductive composite layer at 80 kPa is illustrated in Figure 3d. Notably, when the sensor thickness is 1 mm, the

sensitivity is at its highest. As the sensor thickness increases, the piezoresistive sensitivity diminishes due to the thinner piezoresistive layer, resulting in a greater relative deformation of the sensor under the same pressure conditions. It is also evident that, following the application of the same pressure, the sensor's resistance remains stable.

3.4. Sensing Performance of Piezoresistive Sensors.
Based on the comparative analysis of sensor performance under various parameters, we determined that the composite conductive filler, composed of 87% SAP, 10% absorbed phosphoric acid, and 3% CNT doping, yielded optimal results. This composite conductive filler was combined with the PDMS reagent in a 3:2 ratio to create the piezoresistive layer of the sensor, and its pressure measurement performance was evaluated, as depicted in Figure 4a. The experimental test system is shown in Figure S4. Sensitivity (S) is mathematically expressed as $S = \delta(\Delta R)/\delta P$, where $\delta(\Delta R)$ represents the change in resistance and δP represents the change in applied pressure. Given that resistance decreases with increasing pressure, for ease of comparison, we consider ΔR as positive by taking its absolute value. By calculation of the slope of the curve, the sensitivity is determined. The sensor's resistance primarily changes due to alterations in the length and the number of conductive paths within the piezoresistive layer. In the 0−2 kPa measurement range, S_1 is 0.094 kPa^{-1}; within the 2−10 kPa range, S_2 is 0.044 kPa^{-1}; and for the 10−150 kPa range, S_3 is 0.0032 kPa^{-1}.

When the flexible piezoresistive sensor is subjected to a slight pressure, the increased pressure leads to rapid fluctuations in the contact number and contact area between the composite conductive particles. The resistance change of the sensor primarily originates from the reduction in the length of the conductive paths within the composite material and an increase in the number of paths, thus rendering it highly sensitive in the low-pressure region. As the flexible piezoresistive sensor encounters higher pressure, the number of conductive paths in the composite material tends to reach saturation. The compressibility of the material gradually decreases, leading to a reduction in the conductive path. Consequently, the sensor's resistance change is primarily attributable to the enlargement of the contact area between the conductive particles, resulting in a lower sensitivity in the high-pressure region.

In the assessment of sensor performance, one crucial metric is the rapid dynamic response to pressure. This is evaluated by applying a weight of 0.1 kg to the sensor, equivalent to 10 kPa of pressure, and subsequently allowing it to remain in place for a specified duration before the weight. The data recorded by the sensor throughout this process are depicted in Figure 4b, showcasing a response time of 105 ms and a relaxation time of 194 ms. These findings underscore the sensor's capacity for swift responsiveness, enabling it to promptly detect pressure variations within a short time frame and rapidly revert to its baseline state after pressure relief. Such characteristics are of paramount importance in real-time pressure measurements across a multitude of application scenarios. The static response to pressure represents another vital parameter for assessing the sensor performance. As illustrated in Figure 4c, a continuous response curve of relative resistance changes was generated by monitoring the loading and unloading processes of the sensor under various pressure levels. These curves serve to delineate and stabilize performance characteristics, offering indispensable insights into sensor reliability and accuracy.

As depicted in Figure 4d, even after 5000 cycles, the sensor continues to exhibit outstanding mechanical stability while consistently presenting a resistance change curve. This remarkable stability owes itself to the meticulous blending of the composite conductive filler, SPC, and the PDMS matrix. This precise proportioning ensures both the conductivity and elasticity of the piezoresistive layer. Sensors incorporating this composite conductive layer maintain exceptional signal stability even after enduring a substantial number of load and unload cycles. To assess the dynamic response speed of the sensor, it was subjected to a compression of 10 kPa and tested in a cyclic manner at a frequency of 0.5 Hz. These results illustrate that the sensor is capable of rapid responses even under high-frequency compression, further underscoring its reliability and performance in dynamic applications.

Furthermore, as illustrated in Figure 4e, piezoresistive sensors utilizing composite conductive fillers exhibit an impressively low detection limit, well below 5 Pa. The blue curve represents the resistance change trend with data collected by a digital source meter, while the orange curve depicts the pressure application process with data obtained from the tension sensor. Observing the right side of Figure 4e, it can be deduced that when the pressure reaches or exceeds 2 Pa, the pressure change curve aligns closely with the resistance change curve. Therefore, based on the data from this study, the detection limit is confirmed to be below 5 Pa. Nevertheless, at low-pressure levels, minor airflow or ambient vibrations may introduce inaccuracies in sensor measurements. Additionally, in the conditions of high sampling frequency used in the experiments, some noise points may appear, potentially influencing the curve's consistency. Given the sensor's wide measurement range, the 5 Pa detection lower limit suffices for the demands of its intended application environment, obviating the need for further precise experiments to verify the detection limit.

Figure 4f presents the stress−strain curves of the piezoresistive layer comprising the composite conductive filler under various compressive strains. It is evident that the sensor layer displays typical elastomeric behavior when subjected to low-amplitude, rubber-like deformations. Under high-amplitude deformations, the stress release curve of the piezoresistive layer almost returns to its initial state without plastic deformation. These findings demonstrate that the composite conductive filler employed in this study can withstand substantial mechanical deformations and exhibits excellent resilience during the release of compressive stress.

The composition of the composite conductive filler exhibits relative stability and is not easily influenced by environmental factors or the passage of time. These constituents encompass PDMS polymers and CNTs, both of which are known for their extended service life and resistance to decomposition or degradation. Consequently, the pressure sensor fabricated herein demonstrated sustained performance stability over a period of 2 weeks, as depicted in Figure 4g. In comparison with the published literature, as illustrated in Figure 4h, the measurement sensitivity and detection range of the pressure sensor featuring the composite conductive filler, designed in this study, exhibit superior performance.[44−49]

3.5. Application of Sensors and Sensor Networks in Practical Measurements.
The sensor developed in this study exhibits characteristics such as a broad measurement range, high sensitivity, and a low measurement limit. To confirm that the sensor can cater to diverse measurement
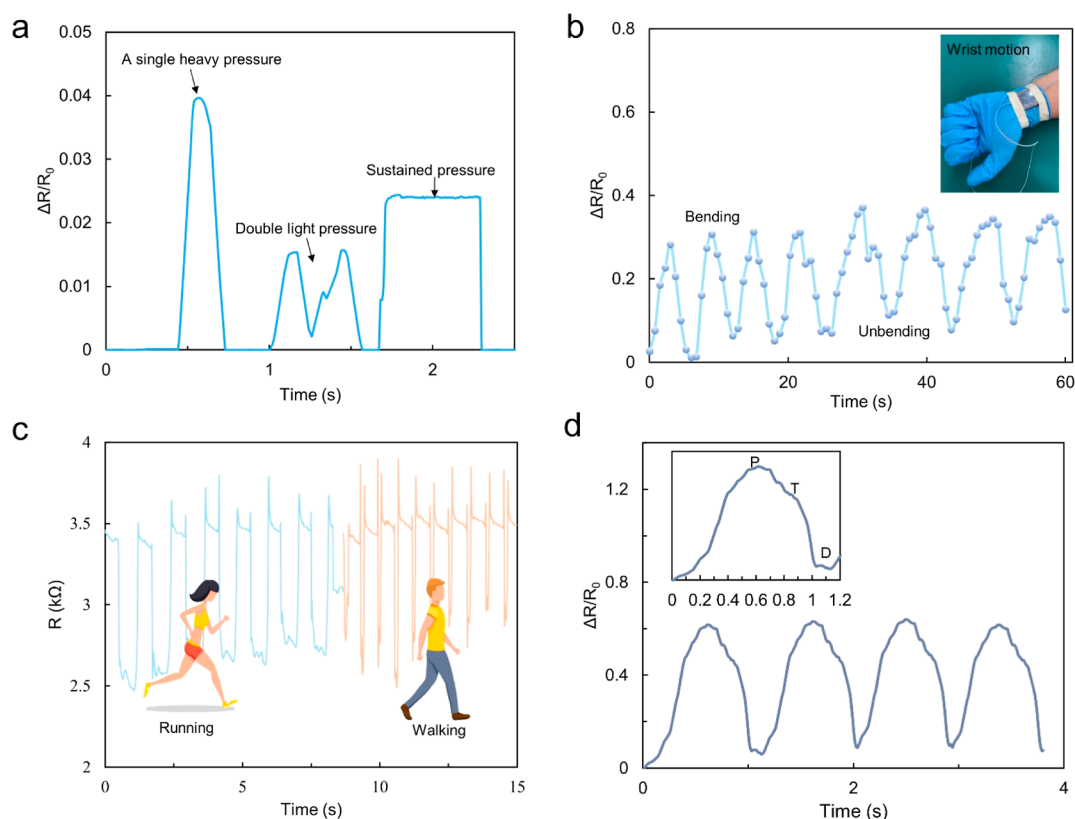
Figure 5. Performance verification test of a flexible piezoresistive sensor. (a) Resistive responses to light and heavy pressing of single and multiple fingers. (b) Wrist bending motion is detected using a piezoresistive sensor. (c) A piezoresistive sensor is used for gait detection. (d) Application demonstration for pulse signal monitoring.

requirements under various conditions, Figure 5 presents the performance of the piezoresistive pressure sensor across different application scenarios. As depicted in Figure 5a, the sensor demonstrates immediate responsiveness to human finger touches and presses, thereby establishing its applicability in a wide array of situations. These scenarios encompass single and repeated presses, both light and heavy, as well as short and prolonged presses.

To provide a more comprehensive demonstration of the sensor's capabilities in real-time monitoring of dynamic stress, we employed the sensor for tracking human movements, with a focus on wrist movements, as exemplified in Figure 5b. Piezoresistive pressure sensors were affixed to the wrist using tape, and they monitored the bending motion of the wrist by recording the relative resistance changes. The experimental findings indicate that the sensor adheres securely to the wrist and effectively captures the bending motion. As the wrist bends, the relative resistance of the sensor increases, and upon the wrist returning to its initial position, the resistance value also reverts to its original level. This underscores the sensor's potential for applications in human motion monitoring, as it reliably captures and records changes during motion.

Gait monitoring, encompassing parameters such as the step length and cadence, represents a promising and distinctive biometric technology. Conventional gait data collection methods involving CCD cameras or acceleration sensors are intricate and cost-intensive. In this context, piezoresistive sensors offer an efficient solution for monitoring the human gait. Given that the human stepping frequency constitutes a low-frequency signal, pressure sensors can precisely capture each movement. As illustrated in Figure 5c, diverse states of

running and walking can be effectively monitored and differentiated. Through the recording of the user's step frequency and pressure per single step within a specific time frame, this technology can serve as a valuable reference for assessing movement posture, enabling users to make necessary adjustments and enhance the efficacy of their physical activities.

Being a crucial physiological indicator of the human body, the pulse serves as a valuable tool for assessing the overall health status and detecting potential disease-related information. Therefore, ensuring the reliable monitoring of pulse signals at each stage stands as a pivotal objective in the pressure sensor design. As depicted in Figure 5d, through the amplification of a single cycle's pulse signal, distinct components such as the P waves (atrial contraction), T waves (ventricular diastole), and D waves (changes in the depolarization potential of the left and right atria) are clearly discernible, aligning with the fundamental pulse signal. Experimental results affirm that the piezoresistive pressure sensor proposed in this study effectively captures pulse signals.

A network of flexible piezoresistive sensors offers a wide array of applications spanning healthcare, wearable technology, automation, robotics, structural health monitoring, and more. Its notable attributes, including sensitivity, adaptability, and cost-effectiveness, render it a potent tool for enhancing the quality of life, boosting productivity, and driving technological innovation. In this research, a piezoresistive sensor network was configured to monitor pressure variations at multiple points. This network comprises a portable LCR acquisition instrument, a programmable logic controller (PLC) module, a power module, and a custom-designed upper computer system,
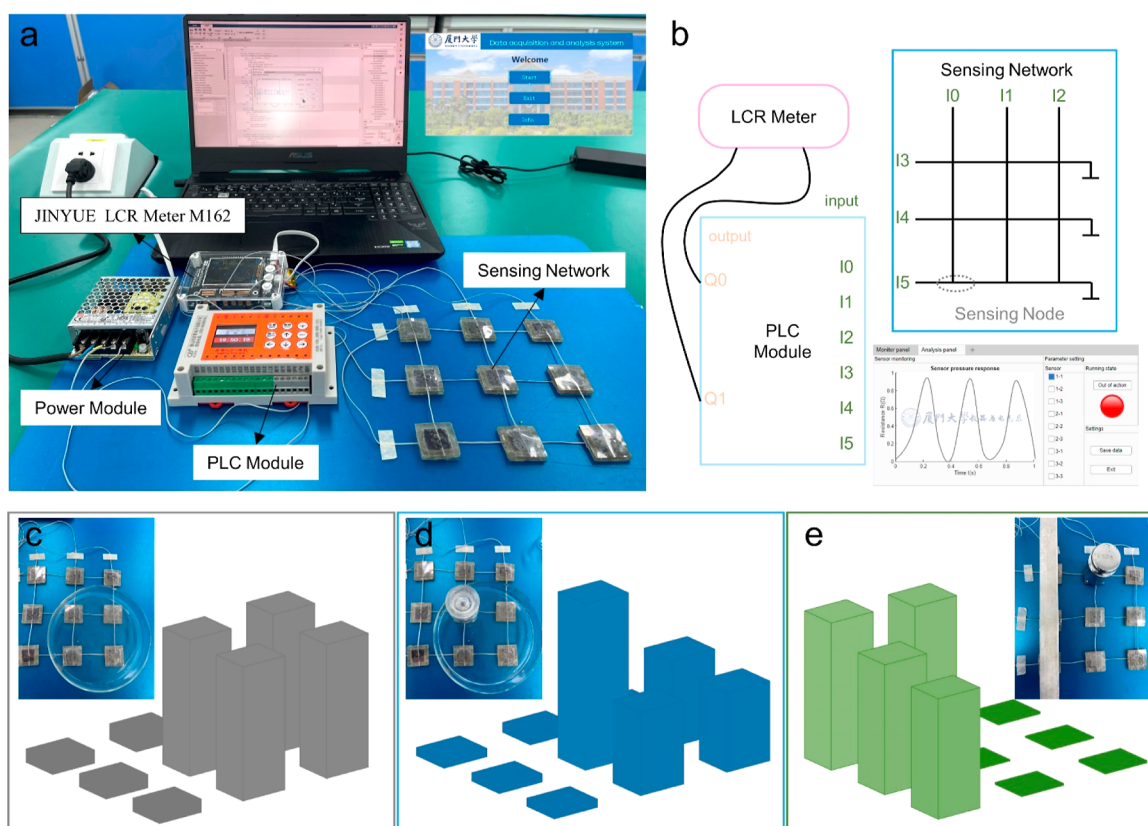
Figure 6. Portable piezoresistive sensing network system. (a) Optical photographs of the sensor network. (b) Acquisition circuit of the sensor network. (c−e) Application verification of the sensing network.

as depicted in Figure 6a. Its primary objective is to enable real-time monitoring of pressure changes at multiple points with the use of multiple sensors. This capability proves crucial for tasks such as studying object weight distribution and touch sensing, among other applications. By integration of the PLC module, the sensor network achieves automatic data acquisition and response, providing robust support for automated production and industrial control. The incorporation of the portable LCR acquisition instrument enables the evaluation and calibration of the sensor performance. The core advantage of this system lies in its capacity for multipoint monitoring, offering significant support for research and practical applications across diverse fields.

The circuit diagram of the sensor network acquisition system is illustrated in Figure 6b. In contrast to the parallel sampling mode, which necessitates multiple measurement and acquisition systems, the multichannel sampling mode requires only a single measurement and sampling system. For a 3 × 3 sensor network organized based on network topology, it requires 3 + 3 wires. However, given that the portable LCR collector features only two acquisition ports, it becomes necessary to sequentially output the signals of all 6 wires through the PLC module. It is important to note that the multichannel sampling mode may introduce interference during the sampling process, potentially impacting measurement accuracy. Furthermore, any failure in the sampling system can affect data collection across multiple measurement points. The upper computer system designed in this study primarily serves three functions: serial port setting and connection, data collection and analysis, and data storage. Within the data analysis segment, the collected data can be

automatically categorized, allowing users to retrieve the desired sensor node's corresponding data through selection.

To substantiate the reliability and accuracy of the sensor network, this study conducted three experiments, the results of which are presented in Figure 6c−e. In Figure 6c, a piece of glassware was positioned on the sensor network, resulting in a uniform stress distribution due to the even distribution of the external forces. In Figure 6d, when glassware was placed at the center of the sensor network, the central section of the network experienced the highest pressure. Lastly, in Figure 6e, when an unevenly distributed pressure was applied using a hammer, the pressure distribution across the sensor network also faithfully mirrored the characteristics of the hammer's impact. These experimental outcomes affirm that the sensor network can accurately detect and reflect external forces, showcasing its reliable performance and its potential for application in diverse scenarios for pressure monitoring.

4. CONCLUSIONS

In summary, this article presents a flexible piezoresistive sensor based on a composite conductive filler. A flexible sensing network is constructed using a portable LCR instrument and a PLC module. The sensor operates on the principle of pressure-induced movement of charge carriers within the conductive filler, forming a conductive pathway and resulting in a change in resistance for pressure detection. The sensor's structure is straightforward, incorporating ITO/PET electrodes, a piezoresistive layer comprising SAP material absorbed in phosphoric acid aqueous solution and doped with CNTs. Effective bonding between the flexible polymer PDMS and the

composite conductive filler significantly enhances sensor stability while reducing its Young's modulus.

Experimental results indicate that increasing the SPC content enhances sensor sensitivity to some extent, although the pressure sensitivity decreases with thicker composite layers. Furthermore, the sensor exhibits high sensitivity ($0.094 \, \text{kPa}^{-1}$), rapid response time (105 ms), and exceptional cyclic load/unload stability (over 5000 cycles). In conclusion, this flexible piezoresistive layer, characterized by a simple and reliable manufacturing process, holds promising application potential in motion monitoring and various other fields.

ASSOCIATED CONTENT

Supporting Information

The Supporting Information is available free of charge at https://pubs.acs.org/doi/10.1021/acsomega.3c07945.

> Additional experimental details, materials, and methods, including SEM image after precipitation of metal salt ions, changes in the conductive pathway before and after pressure application, multiple validations of sensor sample preparation reproducibility, and experimental system figures (PDF)

AUTHOR INFORMATION

Corresponding Authors

Xiaofeng Yang — *Science and Technology on Reliability Physics and Application of Electronic Component Laboratory, The Fifth Electronics Research Institute of the Ministry of Industry and Information Technology, Guangzhou 511370, China*; Email: yangxiaofeng@ceprei.com

Hu Sun — *School of Aerospace Engineering, Xiamen University, Xiamen 361005, China*; orcid.org/0000-0002-4272-3552; Email: sunhu@xmu.edu.cn

Authors

Leijin Fan — *School of Aerospace Engineering, Xiamen University, Xiamen 361005, China*; orcid.org/0000-0002-7315-3257

Yuantao Liu — *School of Aerospace Engineering, Xiamen University, Xiamen 361005, China*

Complete contact information is available at:
https://pubs.acs.org/10.1021/acsomega.3c07945

Author Contributions

L.F. performed the data curation, formal analysis, and writing—original draft; Y.L. carried out the experiment implementation, data curation, and formal analysis; X.Y. executed the methodology, formal analysis, and editing; H.S. completed the writing—review, financial support, and supervision. All authors discussed the results and commented on the manuscript.

Notes

The authors declare no competing financial interest.

ACKNOWLEDGMENTS

REFERENCES

(1) Lei, D.; Liu, N.; Su, T.; Zhang, Q.; Wang, L.; Ren, Z.; Gao, Y. Roles of Mxene in Pressure Sensing: Preparation, Composite Structure Design, and Mechanism. *Adv. Mater.* **2022**, *34* (52), 2110608.

(2) Shi, Z.; Meng, L.; Shi, X.; Li, H.; Zhang, J.; Sun, Q.; Liu, X.; Chen, J.; Liu, S. Morphological Engineering of Sensing Materials for Flexible Pressure Sensors and Artificial Intelligence Applications. *Nano-Micro Lett.* **2022**, *14* (1), 141.

(3) Nie, K.; Hou, Q. Applications of negative permeability metamaterials for electromagnetic resonance type wireless power transfer systems. *EPJ Appl. Metamat.* **2023**, *10*, 2.

(4) Fan, G.; Sun, K.; Hou, Q.; Wang, Z.; Liu, Y.; Fan, R. Epsilon-negative media from the viewpoint of materials science. *EPJ Appl. Metamat.* **2021**, *8*, 11.

(5) Lu, J.; Jing, J.; Zhou, X.; Han, G.; Zhang, Z.; Gong, H.; Wang, X.; Wang, G.; Miao, Y.; Sheng, M.; Liu, M. Vat photopolymerization 3D printing gyroid meta-structural SiOC ceramics achieving full absorption of X-band electromagnetic wave. *Addit. Manuf.* **2023**, *78*, 103827.

(6) Sundaram, S.; Kellnhofer, P.; Li, Y.; Zhu, J.-Y.; Torralba, A.; Matusik, W. Learning the Signatures of the Human Grasp Using a Scalable Tactile Glove. *Nature* **2019**, *569* (7758), 698−702.

(7) Baek, S.; Lee, Y.; Baek, J.; Kwon, J.; Kim, S.; Lee, S.; Strunk, K.-P.; Stehlin, S.; Melzer, C.; Park, S.-M.; et al. Spatiotemporal Measurement of Arterial Pulse Waves Enabled by Wearable Active-Matrix Pressure Sensor Arrays. *ACS Nano* **2022**, *16* (1), 368−377.

(8) Fan, L.; Yang, X.; Sun, H. A Novel Flexible Sensor for Double-Parameter Decoupling Measurement of Temperature and Pressure with High Sensitivity and Wide Range. *J. Mater. Chem. C* **2023**, *11* (30), 10163−10177.

(9) Fiorillo, A. S.; Critello, C. D.; Pullano, S. A. Theory, Technology and Applications of Piezoresistive Sensors: A Review. *Sens. Actuators, A* **2018**, *281*, 156−175.

(10) Mishra, R. B.; El-Atab, N.; Hussain, A. M.; Hussain, M. M. Flexible Capacitive Pressure Sensors: Recent Progress on Flexible Capacitive Pressure Sensors: From Design and Materials to Applications. *Adv. Mater. Technol.* **2021**, *6* (4), 2001023.

(11) Tang, T.; Shen, Z.; Wang, J.; Xu, S.; Jiang, J.; Chang, J.; Guo, M.; Fan, Y.; Xiao, Y.; Dong, Z.; et al. Stretchable Polymer Composites with Ultrahigh Piezoelectric Performance. *Natl. Sci. Rev.* **2023**, *10* (8), nwad177.

(12) He, J.; Xie, Z.; Yao, K.; Li, D.; Liu, Y.; Gao, Z.; Lu, W.; Chang, L.; Yu, X. Trampoline Inspired Stretchable Triboelectric Nano-generators as Tactile Sensors for Epidermal Electronics. *Nano Energy* **2021**, *81*, 105590.

(13) Xu, S.; Xu, Z.; Li, D.; Cui, T.; Li, X.; Yang, Y.; Liu, H.; Ren, T. Recent Advances in Flexible Piezoresistive Arrays: Materials, Design, and Applications. *Polymers* **2023**, *15* (12), 2699.

(14) Pierre Claver, U.; Zhao, G. Recent Progress in Flexible Pressure Sensors Based Electronic Skin. *Adv. Eng. Mater.* **2021**, *23* (5), 2001187.

(15) He, J.; Zhang, Y.; Zhou, R.; Meng, L.; Chen, T.; Mai, W.; Pan, C. Recent Advances of Wearable and Flexible Piezoresistivity Pressure Sensor Devices and Its Future Prospects. *J. Mater.* **2020**, *6* (1), 86−101.

(16) Huang, Y.; Fan, X.; Chen, S.-C.; Zhao, N. Emerging Technologies of Flexible Pressure Sensors: Materials, Modeling, Devices, and Manufacturing. *Adv. Funct. Mater.* **2019**, *29* (12), 1808509.

(17) He, F.; You, X.; Wang, W.; Bai, T.; Xue, G.; Ye, M. Recent Progress in Flexible Microstructural Pressure Sensors toward Human-Machine Interaction and Healthcare Applications. *Small Methods* **2021**, *5* (3), 2001041.

(18) Haghgoo, M.; Hassanzadeh-Aghdam, M. K.; Ansari, R. A Comprehensive Evaluation of Piezoresistive Response and Percolation Behavior of Multiscale Polymer-Based Nanocomposites. *Composites, Part A* **2020**, *130*, 105735.

(19) Bauhofer, W.; KovACS, J. Z. A Review and Analysis of Electrical Percolation in Carbon Nanotube Polymer Composites. *Compos. Sci. Technol.* **2009**, *69* (10), 1486−1498.

(20) Zhai, Y.; Yu, Y.; Zhou, K.; Yun, Z.; Huang, W.; Liu, H.; Xia, Q.; Dai, K.; Zheng, G.; Liu, C.; et al. Flexible and Wearable Carbon Black/Thermoplastic Polyurethane Foam with a Pinnate-Veined Aligned Porous Structure for Multifunctional Piezoresistive Sensors. *Chem. Eng. J.* **2020**, *382*, 122985.

(21) Wang, L.; Peng, H.; Wang, X.; Chen, X.; Yang, C.; Yang, B.; Liu, J. Pdms/Mwcnt-Based Tactile Sensor Array with Coplanar Electrodes for Crosstalk Suppression. *Microsyst. Nanoeng.* **2016**, *2*, 16065.

(22) Zhang, S.; Liu, H.; Yang, S.; Shi, X.; Zhang, D.; Shan, C.; Mi, L.; Liu, C.; Shen, C.; Guo, Z. Ultrasensitive and Highly Compressible Piezoresistive Sensor Based on Polyurethane Sponge Coated with a Cracked Cellulose Nanofibril/Silver Nanowire Layer. *ACS Appl. Mater. Interfaces* **2019**, *11* (11), 10922−10932.

(23) Han, X.; Lv, Z.; Ran, F.; Dai, L.; Li, C.; Si, C. Green and Stable Piezoresistive Pressure Sensor Based on Lignin-Silver Hybrid Nanoparticles/Polyvinyl Alcohol Hydrogel. *Int. J. Biol. Macromol.* **2021**, *176*, 78−86.

(24) Yan, J.; Ma, Y.; Jia, G.; Zhao, S.; Yue, Y.; Cheng, F.; Zhang, C.; Cao, M.; Xiong, Y.; Shen, P.; et al. Bionic Mxene Based Hybrid Film Design for an Ultrasensitive Piezoresistive Pressure Sensor. *Chem. Eng. J.* **2022**, *431*, 133458.

(25) Qin, Z.; Lv, Y.; Fang, X.; Zhao, B.; Niu, F.; Min, L.; Pan, K. Ultralight Polypyrrole Crosslinked Nanofiber Aerogel for Highly Sensitive Piezoresistive Sensor. *Chem. Eng. J.* **2022**, *427*, 131650.

(26) Li, L.; Bao, X.; Meng, J.; Zhang, C.; Liu, T. Sponge-Hosting Polyaniline Array Microstructures for Piezoresistive Sensors with a Wide Detection Range and High Sensitivity. *ACS Appl. Mater. Interfaces* **2022**, *14* (26), 30228−30235.

(27) Shi, L.; Li, Z.; Chen, M.; Qin, Y.; Jiang, Y.; Wu, L. Quantum Effect-Based Flexible and Transparent Pressure Sensors with Ultra-high Sensitivity and Sensing Density. *Nat. Commun.* **2020**, *11* (1), 3529.

(28) Tang, Z.; Jia, S.; Zhou, C.; Li, B. 3d Printing of Highly Sensitive and Large-Measurement-Range Flexible Pressure Sensors with a Positive Piezoresistive Effect. *ACS Appl. Mater. Interfaces* **2020**, *12* (25), 28669−28680.

(29) Gao, Y.; Lu, C.; Guohui, Y.; Sha, J.; Tan, J.; Xuan, F. Laser Micro-Structured Pressure Sensor with Modulated Sensitivity for Electronic Skins. *Nanotechnology* **2019**, *30* (32), 325502.

(30) Park, J.; Kim, J.; Hong, J.; Lee, H.; Lee, Y.; Cho, S.; Kim, S.-W.; Kim, J. J.; Kim, S. Y.; Ko, H. Tailoring Force Sensitivity and Selectivity by Microstructure Engineering of Multidirectional Electronic Skins. *NPG Asia Mater.* **2018**, *10*, 163−176.

(31) Li, H.; Wu, K.; Xu, Z.; Wang, Z.; Meng, Y.; Li, L. Ultrahigh-Sensitivity Piezoresistive Pressure Sensors for Detection of Tiny Pressure. *ACS Appl. Mater. Interfaces* **2018**, *10* (24), 20826−20834.

(32) Chen, M.; Li, K.; Cheng, G.; He, K.; Li, W.; Zhang, D.; Li, W.; Feng, Y.; Wei, L.; Li, W.; et al. Touchpoint-Tailored Ultrasensitive Piezoresistive Pressure Sensors with a Broad Dynamic Response Range and Low Detection Limit. *ACS Appl. Mater. Interfaces* **2019**, *11* (2), 2551−2558.

(33) Niu, H.; Zhang, H.; Yue, W.; Gao, S.; Kan, H.; Zhang, C.; Zhang, C.; Pang, J.; Lou, Z.; Wang, L.; et al. Micro-Nano Processing of Active Layers in Flexible Tactile Sensors Via Template Methods: A Review. *Small* **2021**, *17* (41), 2100804.

(34) dos Santos, A.; Pinela, N.; Alves, P.; Santos, R.; Fortunato, E.; Martins, R.; Aguas, H.; Igreja, R. Piezoresistive E-Skin Sensors Produced with Laser Engraved Molds. *Adv. Electron. Mater.* **2018**, *4* (9), 1800182.

(35) Yao, H.; Yang, W.; Cheng, W.; Tan, Y. J.; See, H. H.; Li, S.; Ali, H. P. A.; Lim, B. Z. H.; Liu, Z.; Tee, B. C. K. Near-Hysteresis-Free Soft Tactile Electronic Skins for Wearables and Reliable Machine Learning. *Proc. Natl. Acad. Sci. U.S.A.* **2020**, *117* (41), 25352−25359.

(36) Pang, Y.; Zhang, K.; Yang, Z.; Jiang, S.; Ju, Z.; Li, Y.; Wang, X.; Wang, D.; Jian, M.; Zhang, Y.; et al. Epidermis Microstructure Inspired Graphene Pressure Sensor with Random Distributed Spinosum for High Sensitivity and Large Linearity. *ACS Nano* **2018**, *12* (3), 2346−2354.

(37) Du, D.; Ma, X.; An, W.; Yu, S. Flexible Piezoresistive Pressure Sensor Based on Wrinkled Layers with Fast Response for Wearable Applications. *Measurement* **2022**, *201*, 111645.

(38) Fan, L.; Yang, X.; Sun, H. Pressure Sensors Combining Porous Electrodes and Electrospun Nanofiber-Based Ionic Membranes. *ACS Appl. Nano Mater.* **2023**, *6* (5), 3560−3571.

(39) Tee, B. C. K.; Wang, C.; Allen, R.; Bao, Z. An Electrically and Mechanically Self-Healing Composite with Pressure- and Flexion-Sensitive Properties for Electronic Skin Applications. *Nat. Nanotechnol.* **2012**, *7* (12), 825−832.

(40) He, Z.; Byun, J.-H.; Zhou, G.; Park, B.-J.; Kim, T.-H.; Lee, S.-B.; Yi, J.-W.; Um, M.-K.; Chou, T.-W. Effect of Mwcnt Content on the Mechanical and Strain-Sensing Performance of Thermoplastic Polyurethane Composite Fibers. *Carbon* **2019**, *146*, 701−708.

(41) Wang, Y.; Jia, K.; Zhang, S.; Kim, H. J.; Bai, Y.; Hayward, R. C.; Suo, Z. Temperature Sensing Using Junctions between Mobile Ions and Mobile Electrons. *Proc. Natl. Acad. Sci. U.S.A.* **2022**, *119* (4), No. e2117962119.

(42) Wang, Y. C.; Xie, S. J.; Bai, Y.; Suo, Z. G.; Jia, K. Transduction between Magnets and Ions. *Mater. Horiz.* **2021**, *8* (7), 1959−1965.

(43) Kim, H. J.; Chen, B. H.; Suo, Z. G.; Hayward, R. C. Ionoelastomer Junctions between Polymer Networks of Fixed Anions and Cations. *Science* **2020**, *367* (6479), 773−776.

(44) Mannsfeld, S. C. B.; Tee, B. C. K.; Stoltenberg, R. M.; Chen, C. V. H. H.; Barman, S.; Muir, B. V. O.; Sokolov, A. N.; Reese, C.; Bao, Z. Highly Sensitive Flexible Pressure Sensors with Microstructured Rubber Dielectric Layers. *Nat. Mater.* **2010**, *9* (10), 859−864.

(45) Song, Y.; Chen, H.; Su, Z.; Chen, X.; Miao, L.; Zhang, J.; Cheng, X.; Zhang, H. Highly Compressible Integrated Super-capacitor-Piezoresistance-Sensor System with Cnt-Pdms Sponge for Health Monitoring. *Small* **2017**, *13* (39), 1702091.

(46) Sheng, L.; Liang, Y.; Jiang, L.; Wang, Q.; Wei, T.; Qu, L.; Fan, Z. Bubble-Decorated Honeycomb-Like Graphene Film as Ultrahigh Sensitivity Pressure Sensors. *Adv. Funct. Mater.* **2015**, *25* (41), 6545−6551.

(47) Qin, Y.; Peng, Q.; Ding, Y.; Lin, Z.; Wang, C.; He, X.; Xu, F.; Li, J.; Yuan, Y.; Li, Y.; et al. Lightweight, Superelastic, and Mechanically Flexible Graphene/Polyimide Nanocomposite Foam for Strain Sensor Application. *ACS Nano* **2015**, *9* (9), 8933−8941.

(48) Chen, S.; Zhuo, B.; Guo, X. Large Area One-Step Facile Processing of Microstructured Elastomeric Dielectric Film for High Sensitivity and Durable Sensing over Wide Pressure Range. *ACS Appl. Mater. Interfaces* **2016**, *8* (31), 20364−20370.

(49) Wang, G.; Yan, J.; Yang, X.; Qing, X. A Flexible Pressure Sensor Based on Composite Piezoresistive Layer. *IEEE Sens. J.* **2022**, *22* (1), 405−411.